

## DMO/AMO in the presence of caustics

*Alison E. Malcolm\*, Maarten V. De Hoop and Jérôme H. Le Rousseau  
Center for Wave Phenomena, Colorado School of Mines*

### Summary

Dip moveout (DMO) and azimuth moveout (AMO) are considered in a general framework that allows for lateral variations in the velocity model, including those which generate caustics in the wavefield. DMO and AMO are constructed through the composition of operators, using the scattering angle and azimuth parameterization. In this parameterization, impulse responses are computed in a gaussian gas lens model. Because of the different parameterization, these impulse responses are somewhat different than those shown traditionally. The results clearly show how errors can be introduced by assuming, for example, a constant velocity-gradient model when the true model is laterally heterogeneous.

### Introduction

Traditional partial stacking operators, such as DMO and AMO, are applied to data sets using a constant velocity (or constant vertical velocity-gradient) model. This is done, on the one hand, because the methods are derived in constant media, and on the other hand, to make the algorithms that apply DMO or AMO to data simpler and more efficient.

In more complex media DMO and AMO, as derived in constant media, cannot be applied because of caustics in the wavefield. Even a small heterogeneity can change the rayfield enough that applying constant-medium DMO or AMO to a data set in several different windows will not avoid errors. Figure 1 shows the complex ray structures that can arise in laterally heterogeneous media.

The transformation-to-zero-offset (TZO) operator is equivalent to applying DMO across an entire data set. This operator is the composition of an imaging Generalized Radon Transform (GRT) [?] and an exploding reflector-modeling operator that includes only the portion of the wavefield from a raypath normal to the reflector. By composing two operators we generate a single operator that has the same result as applying the operators one after another.

The transformation-to-common-azimuth (TCA) operator, which is AMO applied over an entire data set, is the composition of three operators. We model the data using the composition of two of these operators, the first of which models all data and the second of which restricts the first to constant azimuth acquisition. This combined operator is then composed with an imaging GRT. The composition of all three operators results in a mapping from an initial data set into a constant-azimuth data set. We determine conditions under which this operator is im-

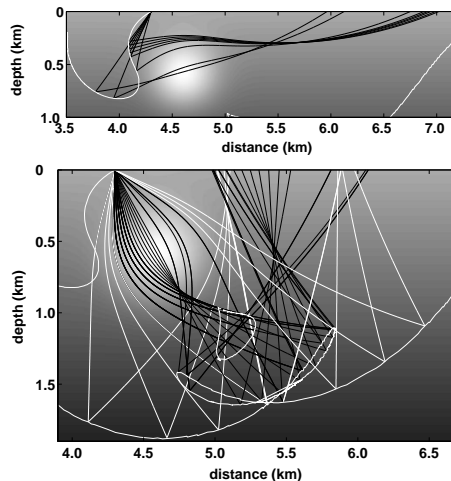


Fig. 1: Depth section showing a model that contains a low-velocity lens, which greatly distorts the rayfield. The white rays come from the outer branch of the isochron (shown in Figure 5) and the black rays come from the inner branches. (Darker shading indicates higher velocity.) The two plots show slightly different regions of the model; both plots use the same source position and scattering angle.

age preserving, i.e., when reflector locations are preserved in the output image.

We develop a framework for analyzing the sensitivity of DMO/AMO with respect to changes in the velocity model. This framework allows one to study the error in applying DMO/AMO in a simplified (typically constant vertical-gradient) velocity model if the true velocity model were to have (strong) lateral variations. These errors will in general be significant since even a small, localized, lateral velocity variation will introduce caustics in the wavefield.

DMO/AMO effectively corresponds to partial stacking, which ideally leads to consistent imaging of reduced (zero-offset or common-azimuth) data sets (computationally efficient because the width of the singular support of the DMO/AMO distribution kernel is small). Conditions under which this imaging is consistent (reflector locations preserved) depend on the properties of the rayfield. It is important to note that rather than extracting a reduced dataset from the entire dataset, DMO/AMO will enhance the signal-to-noise ratio by using all available data in the reduction, exploiting any redundancy in the data.

DMO can also be employed as a tool for velocity analysis. By composing inverse DMO with DMO in a perturbed version of the velocity model it is possible to estimate the

## DMO/AMO in the $\tau$

degree of inconsistency introduced by assuming lateral invariability of the model (residual-velocity DMO [?]).

AMO (as defined in [?]) can be employed to carry out approximate (based on a linearized scattering model) data continuation. Future directions for this work include investigations into using AMO (or similar operators) for data regularization.

### Methodology

Since we consider general velocity models that allow for lateral variations, traditional methods of deriving the necessary operators are insufficient. We use the methods of microlocal analysis to define operators that map our data from one source-receiver configuration to another (e.g., from finite offset to zero offset for DMO).

We construct both the TZO and TCA operators in three steps. First we map data from the acquisition surface to the subsurface. We do this using the angle parameterization and GRT. This allows a model of the subsurface to be constructed from the input data.

Second, we model the desired output data. At this stage we must also ensure that this operator is image preserving, which means that it maps each point in the subsurface to a single point in the data image. If this condition is not met, artifacts may be introduced in the final data.

Finally we must determine whether or not it is possible to compose the two operators and obtain the desired output data. We need to be able to do this in such a way that the information contained in the original data, i.e. the location of reflectors, is preserved in the output data.

In general, both AMO and DMO take as input only a subset of the entire data set. In constant-medium DMO for example, DMO is applied to common-offset data. This restriction of the data to a particular subset generates artifacts in the resulting image. These artifacts can be predicted and filtered out using our methodology. In our parameterization we no longer use as input common-offset data but rather constant-scattering-angle data. Although this is a different subset of the full data set it still retains the same dimensionality as common-offset data.

This same methodology of composing operators can be applied more generally to data regularization, allowing accurate interpolation of missing data in complex media.

### Examples

#### DMO

Traditionally DMO is derived through Fourier methods or using the method of stationary phase [?]. Since we wish to include more general media in our computations we require a more general framework.

The actual TZO operation requires the exploding-reflector modeling operator to be applied to data after the GRT imaging operator discussed above. For the output

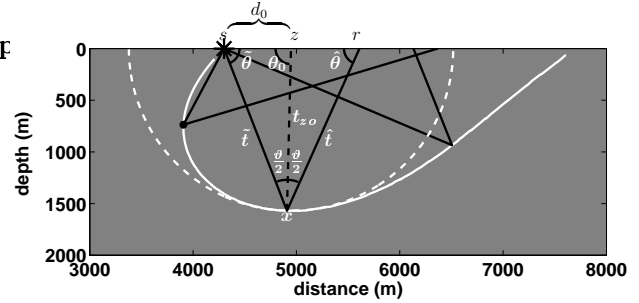


Fig. 2: Notation for the derivation of the constant-medium impulse response. Black lines are rays, the dashed white line is the zero-offset isochron, the solid white line is the angle isochron. The DMO operator maps from the solid isochron to the dashed one.

data from this process to be useful, however, the locations of the reflectors, as seen by the original data, must be preserved. We determine conditions under which this is possible, allowing us to expand the class of models on which TZO can be applied from those with only vertical changes to some containing lateral heterogeneities. These conditions are important to ensure that the output data are accurate. In order to ensure that the resultant image is free of artifacts, however, further filtering would be required.

Under the constant-velocity assumption, DMO is applied to common offset-data, with zero-offset data as the desired output. Since we use the angle parameterization we must find analogous quantities to those used traditionally. We use the source position, scattering angle ( $\vartheta$  in Figure 2) and traveltime in the angle parameterization in place of the midpoint, offset, and traveltime, respectively. Thus to compute the TZO impulse response in the angle domain we fix the source position, scattering angle, and traveltime. It is also interesting to note that, using this more general framework, the problems associated with 3D DMO ([?] p326) disappear because the traditional parameterization of 3D DMO is not well defined in this case. Using the notation defined in Figure 2 one can derive analytically this impulse response for a constant velocity medium, using the law of sines. The resulting relationships are:

$$t_{zo} = \frac{t \sin(\alpha) \sin(\phi)}{(\sin(\alpha) + \sin(\phi)) \sin(\psi)}$$

$$d_{zo} = \frac{ct \sin(\phi) \sin(\frac{\phi}{2})}{(\sin(\alpha) + \sin(\phi)) \sin(\psi)}$$

Figure 3 shows the impulse response derived above;  $t_{zo}$  is plotted as a function of  $d_{zo}$  to match, as closely as possible, the impulse response shown traditionally.

In media with lateral heterogeneities, the impulse response is no longer single valued, as shown in Figure 4, but contains triplications and additional branches. The original structure of the constant medium is visible in this model (note the differences in scale between Figures 3 and

## DMO/AMO in the presence of caustics

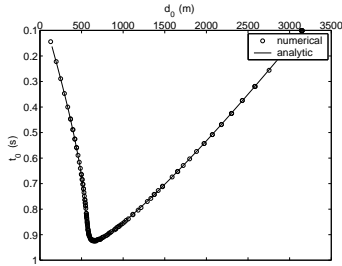


Fig. 3: DMO impulse response for constant-velocity model ( $c=1700$  m/s), as derived above (scattering angle  $45^\circ$ ; time 2 s)

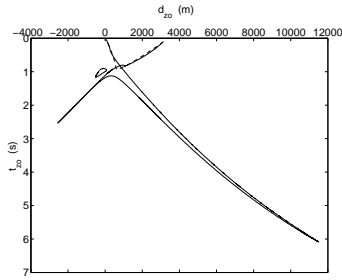


Fig. 4: DMO impulse response for the lens model. The same structures as the constant case are still present but with distortions and additions caused by the lens. The lens model consists of a vertical velocity gradient, beginning at 1700 m/s, and a low velocity lens.

4) but it has been greatly distorted by the presence of the lens. The model used in these figures is the lens model discussed in [?] and consists of a constant vertical velocity gradient with a low velocity ‘gas’ lens. The model is shown in Figure 5.

In Figure 5 it is easy to see where errors can arise. If a constant-gradient DMO were applied to data collected over an Earth that looks more like the lens model than a constant-gradient model, the depth point from which the zero-offset ray originates would be on the solid line rather than the dashed one. In the region below and to the left of the lens, this will result in a large travelttime error since the two lines are relatively far apart. Even after DMO has been incorrectly applied, however, it is possible to reapply a small residual DMO operator, similar to [?], that will undo the initial DMO application and apply a new DMO with lateral variations taken into account. Much of the intermediate computations can be avoided by first computing a combined inverse/forward DMO operator for the particular situation and then applying the smaller resulting operator to the data.

## AMO

The AMO case is quite similar to the DMO case; however, since AMO is inherently 3D while DMO is easily reduced to 2D, the resulting analysis is somewhat more complex.

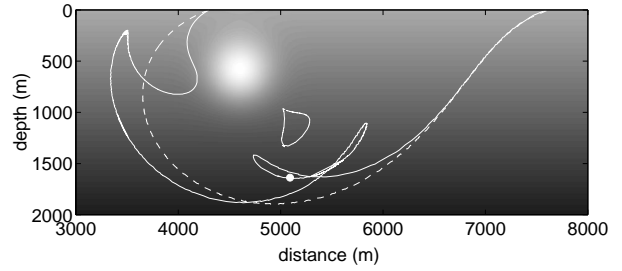


Fig. 5: Angle isochron (source location 4300 m, scattering angle  $45^\circ$ , and time 2 s). The white line shows the isochron from the lens model, and the dashed line is computed in the constant-gradient model with the lens removed. The lens model is shown in the background; darker color indicates higher velocity.

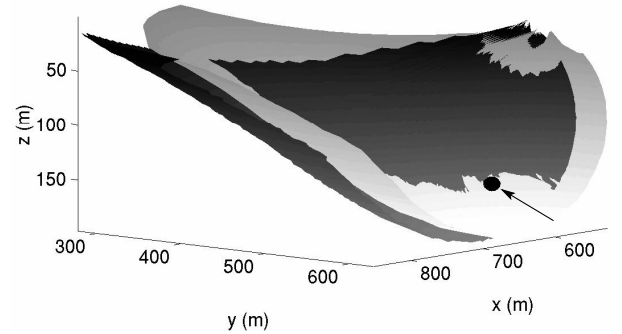


Fig. 6: Illustration of the AMO operator. AMO maps from one isochron to the other by matching points and tangent planes. This figure is similar to Figure 2 in that it shows two isochrons between which the AMO operator maps. The darker isochron is the input isochron and the lighter is the output isochron. The sphere (marked with an arrow) is the point at which the isochrons cross and their tangent planes match.

In translating AMO to the angle domain, we now require a variable to take the place of azimuth in the traditional parameterization (the third dimension). This role is filled by the azimuthal angle between the source and receiver ray directions.

The impulse response and the 3D isochrons will again look different in the angle domain than in the midpoint-offset domain (the impulse response in the midpoint-offset domain is shown in [?]). The isochron in the angle domain shows a shape similar to that in the DMO case, with the expected extension to 3D. Figure 6 shows the construction of the AMO operator as a mapping from one isochron to another in the angle domain. In [?] the AMO impulse response was shown to have a saddle structure, and Figure 7 shows that the structure in the angle domain is somewhat similar. It is once again possible to compute the impulse response analytically in a constant model; however, this computation is more complex so only the resulting figures are shown here.

Once again the gaussian lens introduces complications in the structures of both the impulse response and the

## DMO/AMO in the presence of caustics

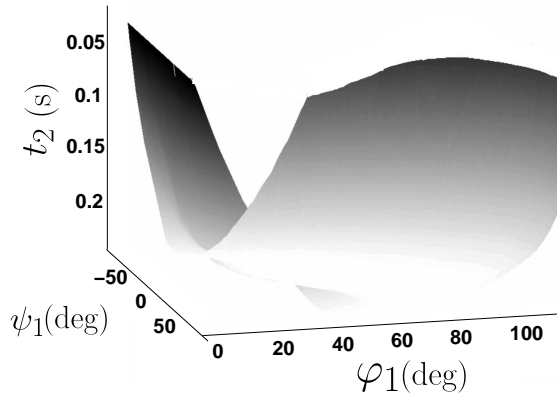


Fig. 7: Plot of the impulse response as a function of input ray directions for AMO;  $\phi_1$  is the angle below the surface, and  $\psi_1$  is the surface azimuthal angle of the source ray.

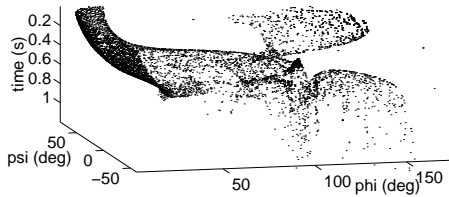


Fig. 8: Surface of the impulse response in the lens model (compare to Figure 7). The lens has again introduced triplications on the surface. Each point on the impulse response is shown here because the triplications present in the lens model are more difficult to see on an interpolated surface.

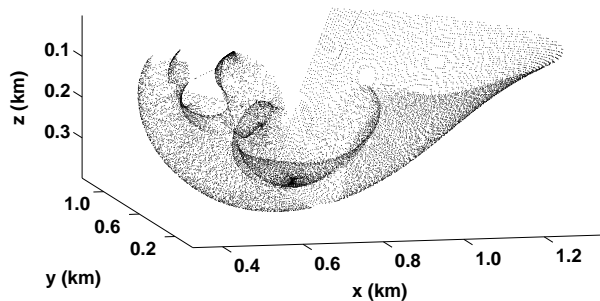


Fig. 9: Surface of the isochron in the lens (compare to Figure 6). Again each point is plotted rather than an interpolated surface.

isochron. These surfaces are shown in Figures 8 and 9. For both, the impulse response (Figure 8) and the isochron, (Figure 9) the lens introduces a multivaluedness to the surfaces as well as distorts the original shape. For both DMO and AMO, the lens also increases the range of the output time and the depth of the isochron. This is mainly due to the vertical gradient, which introduces turning rays into the rayfield that travel for a much larger time than do the straight rays where velocity is constant.

## Conclusions

When applying TZO or TCA to a data set it is important to understand the effects of lateral variations in the Earth on the computed output data. The impulse responses shown in this abstract indicate clearly that lateral variations can result in large errors in the positioning of the scattering point from which the output data set is computed. This is equivalent to a large error in the reflector position because the scattering point is assumed to be on a reflector.

Although artifacts generated in the DMO/AMO process will be less of an issue when the transformation is applied over a complete data set, in order to avoid any artifacts at all it is necessary to use as input data a small range of scattering angles. This range allows the design of a filter to remove artifacts from the final image.

Since AMO/DMO are currently used as tools in regularizing and resampling data, an obvious extension of this work is to investigate data continuation and conditions under which it can be carried out.

## Acknowledgements

This work was supported by the sponsors of the Consortium Project on Seismic Inverse Methods for Complex Structures at the Center for Wave Phenomena.